

adjacent to the insulating layer, nor how this distribution depends on various factors whose importance becomes greater as the thickness is reduced. We cannot exclude the possibility that, owing to the smallness of the screening parameters, variations of the order of few atomic layers have strong influence on the potential distribution inside the electrodes and on their contribution to the total capacitance.

Before concluding, we recall that in our preceding letter<sup>1</sup> we suggested that an effect of this kind could be due to a penetration of the superconducting electron wave functions into the insulating layer, i.e., something

like a proximity effect. But we point out that an effect of this kind would exhibit rather weak critical magnetic field of the order, at most, of the critical fields of the Josephson effect. Of course our measurements on the influence of an applied magnetic field seem to exclude such an interpretation.

#### ACKNOWLEDGMENT

We wish to thank U. Baffi for his invaluable help in the preparation of tunneling junctions and in the performance of the experimental runs.

### Flux Flow in Thin Type-I Superconducting Films\*†

PAUL THOLFSEN‡§ AND HANS MEISSNER

*Department of Physics and Cryogenics Center, Stevens Institute of Technology, Hoboken, New Jersey 07030*

(Received 15 February 1969)

Using dc and pulsed currents of 80-nsec duration, the flux-flow resistance has been observed at temperatures  $T \geq 0.9T_c$  in flat films of tin of thickness 440 to 1580 Å in a perpendicular magnetic field  $H_{\perp}$ . At low values of  $H_{\perp}$ , the reduced flow resistivity  $\rho_f/\rho_n$  is given by  $\rho_f/\rho_n = 0.76 [H_{\perp}/H_{c1}(T)]^{3/2}$ , which is in agreement with published data on bulk type-II superconductors. Flux flow is absent at temperatures  $T \leq 0.9T_c$ , and highly nonlinear for a film of 3420 Å thickness. The flux flow starts at a current density  $J_p$  where the flux tubes break free from their pinning centers. The dependence of  $J_p$  on magnetic field and temperature has been investigated both experimentally and theoretically. As the sample current is increased, an instability is observed at a current density  $J_I$ , at which the resistance increases sharply. The dependence of  $J_I$  on magnetic field, temperature, and film thickness has been determined. Close to  $T_c$ , the instability current  $J_I$  is almost independent of thickness and is given by  $J_I = 3.0 \times 10^6 [1 - (T/T_c)^2] [0.9 - H_{\perp}/H_{c1}(T)]$  A/cm<sup>2</sup>. An investigation of the time dependence of the sample voltage indicates the existence of a time constant  $t'$  which, near  $T_c$ , decreases exponentially with current density.  $J_I$  is then defined as the current density at which  $t'$  becomes shorter than the time of observation.

#### I. INTRODUCTION

THE phenomenon of flux-flow resistance<sup>1</sup> has been investigated in the past few years by several workers. Nearly all of this work has dealt with flux flow in various bulk type-II materials.<sup>2-6</sup> More recently

theoretical<sup>7-9</sup> and experimental evidence<sup>10-17</sup> has been offered, implying that thin films of type-I material in a perpendicular magnetic field should behave similarly to type-II materials: The magnetic field penetrates the film in the form of a flux tube lattice of one (or possibly more<sup>9</sup>) flux quanta each.

There are several differences between the thin films and bulk type-II superconductors: The critical fields  $H_{c1}$  at which superconductivity vanishes, are quite small for the thin film case, typically less than 500 G.

\* Based, in part, on a thesis (PT) submitted to the Department of Physics of Stevens Institute of Technology in partial fulfillment of the requirements for the Ph.D. degree.

† Supported in part by the National Science Foundation, in part by the Cryogenics Center through a grant from the DOD Themis program.

‡ Present address: Physics Department, Western Washington State College, Bellingham, Wash.

§ National Science Foundation Trainee.

<sup>1</sup> P. W. Anderson and Y. B. Kim, *Rev. Mod. Phys.* **36**, 39 (1964).

<sup>2</sup> Y. B. Kim, C. F. Hempstead, and A. R. Strnad, *Rev. Mod. Phys.* **36**, 43 (1964).

<sup>3</sup> A. R. Strnad, C. F. Hempstead, and Y. B. Kim, *Phys. Rev. Letters* **13**, 794 (1964).

<sup>4</sup> Y. B. Kim, C. F. Hempstead, and A. R. Strnad, *Phys. Rev.* **139**, A1163 (1965).

<sup>5</sup> D. E. Farrell, J. Dinewitz, and B. S. Chandrasekhar, *Phys. Rev. Letters* **16**, 91 (1966).

<sup>6</sup> W. F. Vinen and A. C. Warren, *Proc. Roy. Soc. (London)* **91**, 399 (1967).

<sup>7</sup> M. Tinkham, *Phys. Rev.* **129**, 2413 (1963).

<sup>8</sup> Kazumi Maki, *Ann. Phys. (N. Y.)* **34**, 363 (1965).

<sup>9</sup> G. Lasher, *Phys. Rev.* **154**, 345 (1967).

<sup>10</sup> M. Tinkham, *Rev. Mod. Phys.* **36**, 268 (1964).

<sup>11</sup> E. Guyon, C. Caroli, and A. Martinet, *J. Phys. (Paris)* **25**, 683 (1964).

<sup>12</sup> G. D. Cody and R. E. Miller, *Phys. Rev. Letters* **16**, 697 (1966).

<sup>13</sup> R. Deltour and M. Tinkham, *Phys. Letters* **23**, 183 (1966).

<sup>14</sup> J. P. Burger, G. Deutscher, E. Guyon, and A. Martinet, *Phys. Rev.* **137**, A853 (1965).

<sup>15</sup> G. K. Chang and B. Serin, *Phys. Rev.* **145**, 274 (1966).

<sup>16</sup> G. D. Cody and R. E. Miller, *Phys. Rev.* **173**, 481 (1968).

<sup>17</sup> R. E. Miller and G. D. Cody, *Phys. Rev.* **173**, 494 (1968).

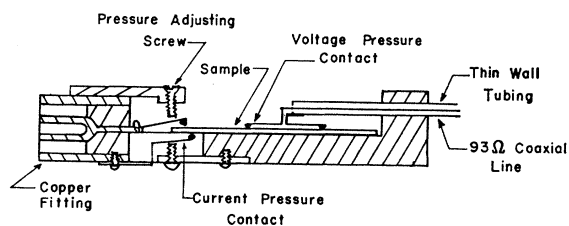


FIG. 1. Sample holder.

Thus all data are taken at rather weak fields and the self-field from the sample current is not necessarily negligibly small. Although the current densities  $J_p$  at which flux tubes break free from pinning centers are relatively high (and the actual pinning forces  $F_p$  are equally high), the corresponding  $I_p$  are relatively small, since the sample cross sections are very small. In the following  $J_p$  or  $I_p$  shall be referred to simply as the "pinning currents." In type-II superconducting materials these pinning currents are usually referred to as  $I_c$ , the critical current.<sup>18</sup>

As will be shown in Sec. V, the flux-flow regime in thin films ends rather abruptly at a current density  $J_I$ , which shall be referred to as the "instability current."

In addition, thin films have a true critical current, which (in zero magnetic field) is given by

$$J_c = (c/4\pi)H_c(T)/\lambda(T), \quad (1)$$

where  $H_c(T)$  is the bulk critical field of the superconductor and  $\lambda(T)$  is the London penetration depth.

Attempts at measuring this critical current have usually resulted<sup>19</sup> in values much smaller than that given by Eq. (1), presumably because the first voltage, taken as the definition for the critical current, occurred at the pinning current (if a small perpendicular component of  $H$ , for instance from the current itself was present accidentally) or at  $J_I$ , the instability current.

By taking thin film strips of less than  $1 \mu\text{m}$  width, too small to contain flux tubes, Hunt<sup>20</sup> was able to obtain stability up to the true critical current.

The discussions above point to the importance of the current return in this type of experiment. It is important that the current return is arranged so as to minimize normal components of the self-field. Such a normal field component will almost always break through the film and will falsify the results at low values of the applied perpendicular field. In this work the current has been returned through a normal conducting film, of the same size as the sample film and at an extremely close distance (0.15 mm).

Another difficulty posed by the experiments with thin films are heating effects. Very close to the critical temperature  $T_c$ , where critical currents and heat inputs are

small, flux-flow resistance measurements can be performed with steady currents. At lower temperatures, however, pulsed currents are necessary. Even then, there is the danger of a "heat wave" traveling along the sample,<sup>21</sup> necessitating extremely short current pulses.

In the present arrangement current pulses of 80-nsec duration have been used. Since the velocity of sound in tin is about  $2.6 \times 10^5 \text{ cm sec}^{-1}$ , a phase boundary moving at the velocity of sound would move during the time of the pulse a distance of about 0.2 mm.

In Sec. II the preparation of the samples and their relevant properties are described. In Sec. III we report data on the pinning currents. In Sec. IV the pulse system and the flux-flow data are described, while in Sec. V the instability current is investigated. Section VI contains a critical discussion, models for the calculation of pinning currents, and concluding remarks.

## II. SAMPLES

The samples were prepared by vacuum deposition of the tin onto 0.15-mm-thick microscope-cover-glass substrates. The substrates were mounted in good thermal contact with a liquid-helium-filled trap. The trap insured that even during evaporation of the tin the pressure did not rise above a few  $10^{-7}$  Torr.

After trimming the edges, the film is about 1.5 mm wide and 5 cm long. The ends are reinforced with a second layer of tin to provide additional strength for the attachment of current and potential leads. The active thin center portion of the film has a length of 14 mm.

After the deposition of the tin, the substrate is turned over and a silver backing film is deposited.

The edges of the sample are then trimmed and it is mounted in the sample holder as shown in Fig. 1. Contacts are made with spring loaded ribbons of manganin (for the potential leads) or phosphor bronze (for the current leads) whose ends contain a dab of tin-indium solder. This solder becomes superconducting at 5.6 K and is mechanically very soft. The lower end of the sample is similarly connected to its backing film. Thus, together with its backing film, the sample forms a shorted strip line with a ratio of width to distance between the films of about ten.

TABLE I. Properties of samples.

Sample	5-1-68	8-24-67	3-8-68	2-18-68
Thickness, Å	440	850	1580	3420
$R_{300}$ , Ω	26.8	9.9	6.2	3.7
$R_{4.2}$ , Ω	2.74	1.12	0.38	0.087
$l_0$ , Å	1 610	1 680	2 140	5 000
$T_c$ , K	3.794	3.794	3.847	3.840
$\lim_{T \rightarrow T_c} \left( -\frac{dH_c}{dT} \right)$ , G	400	455	310	229
$\kappa(1)$	0.47	0.53	0.36	0.27

<sup>18</sup> J. E. Kunzler, Rev. Mod. Phys. **33**, 501 (1961).

<sup>19</sup> J. Mydosh and Hans Meissner, Phys. Rev. **139**, A1920 (1965); and references cited therein.

<sup>20</sup> T. K. Hunt, Phys. Rev. **151**, 325 (1966).

<sup>21</sup> J. W. Bremer and V. L. Newhouse, Phys. Rev. Letters **1**, 282 (1958).

The thickness of the samples was determined to about  $\pm 20 \text{ \AA}$  by multiple beam interferometry on separate samples deposited simultaneously with the main sample.

The samples were mounted in the cryostat, the coaxial system being used both for the pulsed current measurements and for dc measurements.

A small superconducting Helmholtz coil was used to provide a perpendicular field up to 900 G. It was wound from rather soft pure niobium so that the remnant magnetization as well as residual fields were quite small.

The earth's magnetic field was compensated to less than 1% at all times. The temperature of the helium bath was stabilized with an automatic temperature control.<sup>22</sup>

The resistance of the sample was measured at 300 and 4.2 K (see Table I). The latter value was used to find the impurity mean free path  $l_0$  using the equations of Dingle.<sup>23</sup>

Using currents of  $100 \mu\text{A}$ , the resistive transition was recorded as a function of temperature in zero field and as a function of the perpendicular field at several fixed temperatures. The critical temperature  $T_c$  was defined by  $R(T_c) = \frac{1}{2}R_n$ . This eliminated small "tails" of the transition curve on the low-temperature side caused by the thick portions of the film. In a perpendicular magnetic field  $H_1$  this difficulty does not occur and  $H_{c1}$  was defined as the first onset of resistance. Except for the lowest temperatures ( $\sim 1.25 \text{ K}$ ),  $H_{c1}$  varied approxi-

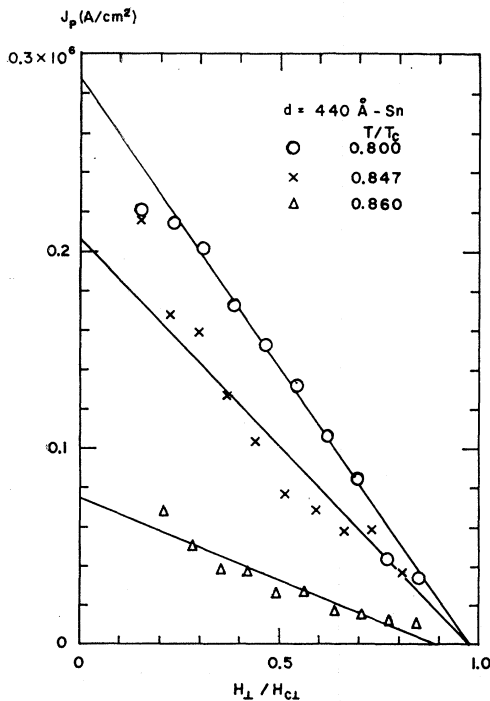


FIG. 2. Dependence of pinning current density  $J_p$  on magnetic field and temperature.

<sup>22</sup> Hans Meissner, Phys. Rev. **109**, 668 (1958).

<sup>23</sup> R. B. Dingle, Proc. Roy. Soc. (London) **A201**, 545 (1950).

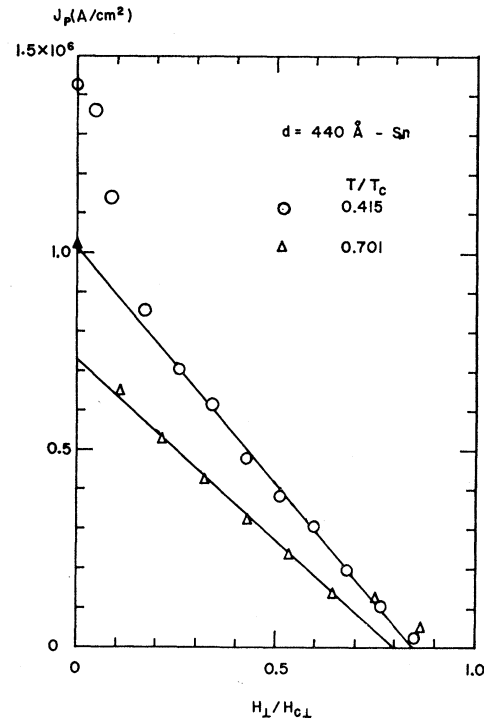


FIG. 3. Dependence of pinning current density  $J_p$  on magnetic field and temperature.

mately linearly with  $T$ . The slopes are given in Table I. This roughly linear dependence is in agreement with Cody and Miller's experimental results<sup>17</sup> and, as they have shown, also with theoretical expectations.<sup>19</sup> The Ginzburg-Landau parameter  $\kappa$  is found from

$$\kappa(T/T_c) = H_{c1}(T)/\sqrt{2}H_c(T); \quad (2)$$

$\kappa$  depends slightly on temperature.<sup>17</sup> Its value  $\kappa(1)$  at  $T/T_c = 1$  is also listed in Table I.

### III. PINNING CURRENTS

The pinning currents were determined by the onset of the voltage on voltage current ( $V$ - $I$ ) plots. Typical  $V$ - $I$  plots with pulsed currents, taken at  $t = 70 \text{ nsec}$  after the start of the current pulse are shown in Sec. IV, Figs. 6-11.

As can be seen, sometimes the onset cannot be determined accurately enough in this way. In these cases special plots were made for the determination of  $I_p$ , using either (near  $T_c$ ) steady currents, or (at intermediate  $T$ ) an enlarged voltage scale. Even with this extra care the definition of  $I_p$  is sometimes slightly arbitrary which makes it difficult to assign error limits.

Figures 2 and 3 show plots of the pinning current density  $J_p$  as a function of  $H_1/H_{c1}(T)$ . For  $0.2H_{c1} \leq H_1 \leq 0.8H_{c1}$  the data points fall roughly on straight lines, so that  $J_p$  can be expressed as

$$J_p = J_{p0}(T/T_c, d)[h_p - H_1/H_{c1}(T)], \quad (3)$$

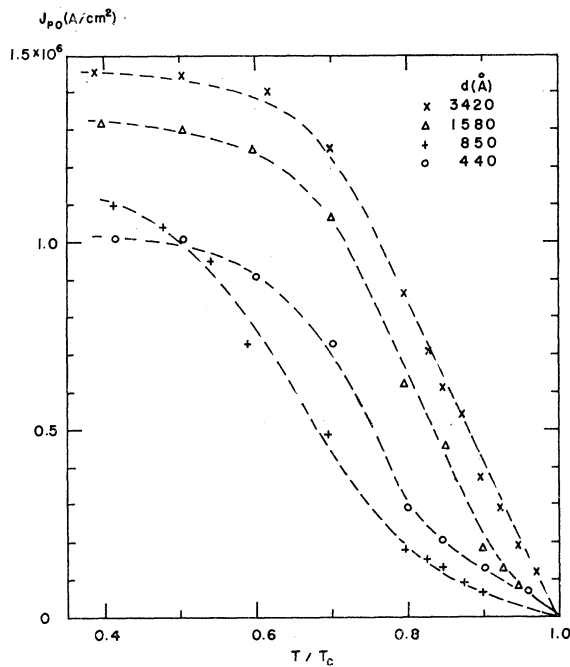


FIG. 4. Dependence of  $J_{p0}$  on temperature and film thickness.

where  $d$  is the film thickness. The values of  $h_p$  range from 0.81 to 0.89. They depend on the definition of  $H_{cl}$ . If the end of the magnetization curve rather than the onset of the resistance had been used for the definition of  $H_{cl}$ , lower values of  $H_{cl}$  and larger values of  $h_p$  would have been found. In view of this it seems reasonable for theoretical discussions to set  $h_p = 1$ .

The dependence of  $J_{p0}(T/T_c, d)$  on temperature and thickness is shown in Fig. 4. Here one has to keep in mind that values of  $J_p > J_I$ , the instability current density, are not observable. It is quite possible that at the lowest temperatures the data points represent  $J_I$  rather than  $J_p$ . Near  $T_c$ , the current  $J_p$  has roughly a

$(T_c - T)^{3/2}$  dependence for the thinnest samples and a  $T_c - T$  dependence for the thickest sample. In comparison with theory, however, one has to keep in mind that experimentally  $J_p$  is very sensitive to disturbing influences: Uniformity of current density and magnetic field, distinction between flux flow and thermally excited flux creep, and sample properties.

IV. FLUX FLOW WITH PULSED CURRENTS

A schematic diagram of the pulse system is shown in Fig. 5. A coaxial cable is charged through a large resistor and is discharged 60 times a second through a coaxially mounted mercury relay to produce 80-nsec repetitive current pulses with a rise time of a few nsec. Two systems were used. One, with a characteristic impedance of 12 Ω, the other with a characteristic impedance of 50 Ω. With a charging voltage from 0.6 to 600 V, the first gave currents from 25 mA to 25 A, while the second gave currents from 6 mA to 6 A. Below 0.6 V charging voltage the triggering of the sampling oscilloscope became uncertain.

Using coaxial thin wall tubes, the pulses are fed to a coaxially mounted alloy film resistor in the helium bath. The sample holder was already described in Sec. II, Fig. 1.

The voltage across the sample is picked up with a coaxial system with an impedance of 93 Ω, terminated in a 93-Ω coaxially mounted resistor. The voltage across the 93-Ω resistor is fed into channel B of the Hewlett Packard Model 185A sampling oscilloscope.

Using an 800-Ω decoupling resistor, the voltage in the main pulse line is picked up on top of the cryostat. This voltage is nearly proportional to the current and is fed through a similar 93-Ω system to channel A of the sampling oscilloscope.

The trigger of the sampling oscilloscope is connected over an 850-Ω uncoupling resistor connected after the relay.

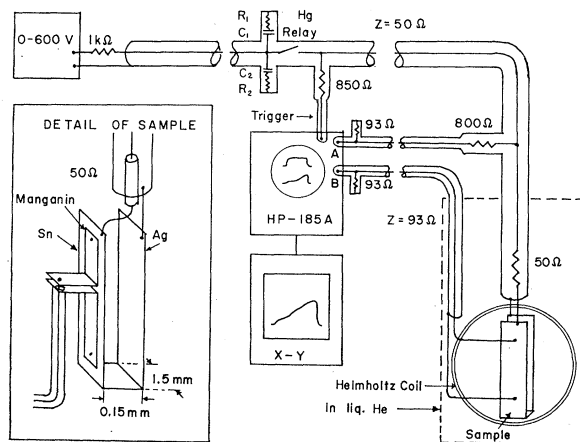


FIG. 5. Pulse system. For explanation, see text.

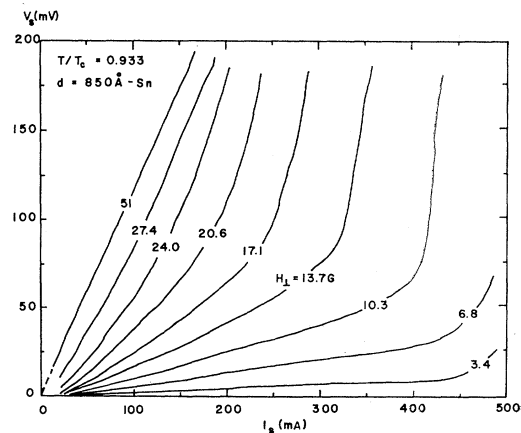


FIG. 6.  $V-I$  characteristic at  $t = 70$  nsec as a function of perpendicular magnetic field.

Suitable lengths of delay are introduced between the relay and the top of the cryostat and in both 93- $\Omega$  systems so that all reflections occur after the end of the pulse.

The pulses are flattened and the rise time is reduced by two coaxial  $RC$  networks connected between center conductor and ground at a point just ahead of the relay.

With this arrangement the following observations are possible:

- The current can be plotted as a function of time,  $I$  versus  $t$ ,
- the sample voltage can be plotted as a function of time  $V$  versus  $t$ ,
- for fixed time, for instance  $t=70$  nsec after the start of the pulse, the voltage can be plotted as a function of the current by varying the charging voltage.

Using the rear terminals of the sampling oscilloscope, all curves can be traced out on the  $L$  &  $N$   $X$ - $Y$  recorder.

A serious problem which arises in fast pulse measurements is the introduction of large induced voltages caused by the large values of  $dI/dt$  occurring during the rise of the pulse. In the present system this voltage  $d\Phi/dt = MdI/dt$  ( $M$  is the mutual inductance between current and potential circuit) is reduced through the use of the strip line configuration and the use of flat ribbons for the potential leads as shown in Fig. 1. The residual  $d\Phi/dt$  voltages were always less than 5% of the  $IR_n$  voltages in the normal state. The "ringing" caused by these voltage spikes disappears after 10 nsec.

The pulse system is easily modified to permit dc measurements as described in Secs. II and III. In the region of overlap, dc and pulse  $V$ - $I$  plots were identical.

Figures 6-10 show a set of  $V$ - $I$  plots for the 850  $\text{\AA}$  sample. At the two higher temperatures  $T/T_c \geq 0.9$  the traces have a distinct linear region, quite similar to the corresponding dc results on bulk type-II samples.<sup>24</sup>

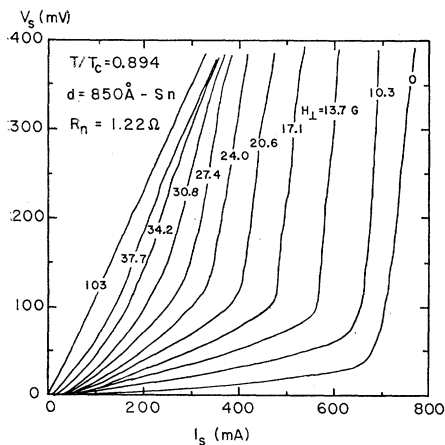


FIG. 7.  $V$ - $I$  characteristic as function of the magnetic field.

<sup>24</sup> R. A. French, J. Lowell, and K. Mendelsohn, *Cryogenics* **7**, 83 (1967).

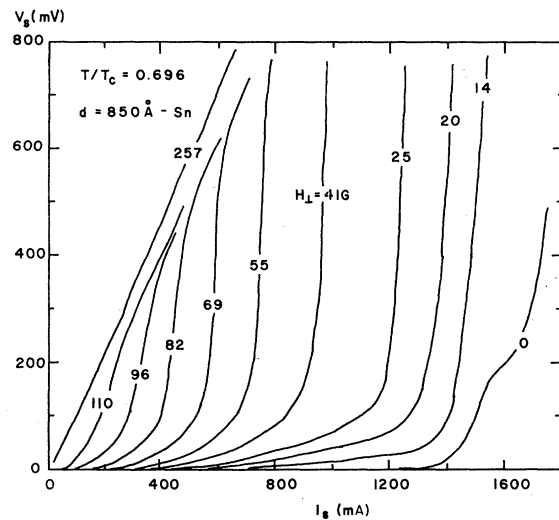


FIG. 8.  $V$ - $I$  characteristic as function of the magnetic field.

The linear portion of each trace ends with an increase in slope, which, at smaller magnetic fields, is quite abrupt. Similar results were obtained for the 440 and 1580  $\text{\AA}$  films. In the case of the 3420  $\text{\AA}$  film, no linear region was obtained, even at relatively high temperatures, as seen in Fig. 11.

This nonlinearity (which in similar experiments has also been found by other observers<sup>13,25</sup>) is most likely caused by the perpendicular component of the magnetic field resulting from the current through the film. For instance on the curve for  $H = 6.9$  G shown in Fig. 11, we expect a linear region from  $I = 0.5$  A to about  $I = 1.3$  A. Assuming that both films (the sample film and its return) have a uniform current distribution, we find that the perpendicular component of the field  $H_T$ , due to

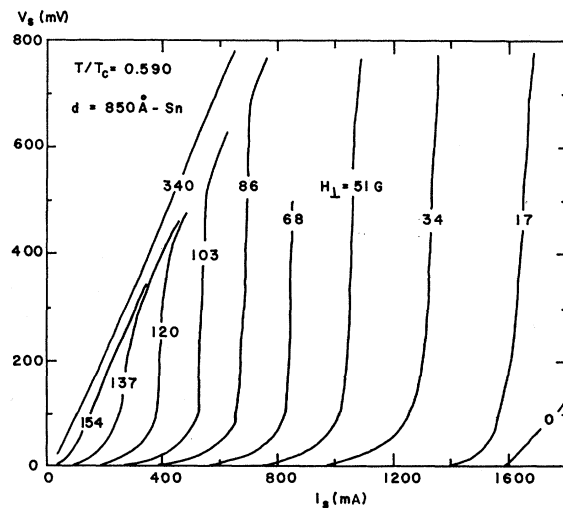


FIG. 9.  $V$ - $I$  characteristic as function of the magnetic field.

<sup>25</sup> P. E. Cladis, *Phys. Rev. Letters* **21**, 1238 (1968).

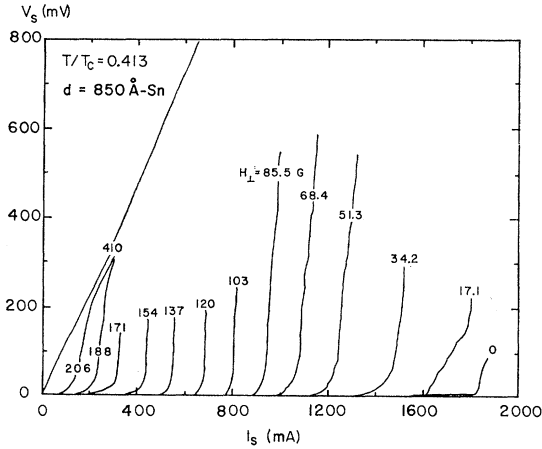


FIG. 10.  $V$ - $I$  characteristic as function of the magnetic field.

the current, has a maximum,  $H_I^{\max}$ , at the edge of the film given by

$$H_I^{\max} = \frac{0.2I}{w} \left[ \left( \ln \frac{w}{d} - 1 \right) - \frac{1}{2} \ln \frac{1 + (2a/w)^2}{(2a/w)^2} \right], \quad (4)$$

where  $w$  is the width of the films,  $d$  their thickness and  $a$  their distance. With  $w = 0.15$  cm,  $a = 1.5 \times 10^{-2}$  cm, and  $d = 3 \times 10^{-5}$  cm,  $H_I^{\max}$  is approximately given by

$$H_I^{\max} = \frac{0.2I}{w} \left( \ln \frac{2a}{d} - 1 \right), \quad (5)$$

where  $I$  is in amperes and  $H_I^{\max}$  is in gauss. For the dimensions given above we find for  $I = 1$  A, that  $H_I^{\max} = 0.788$  G. This is no longer negligibly small compared to the perpendicular field used (6.9 G).

If the current were returned through a tube surrounding the sample, this field would be somewhat

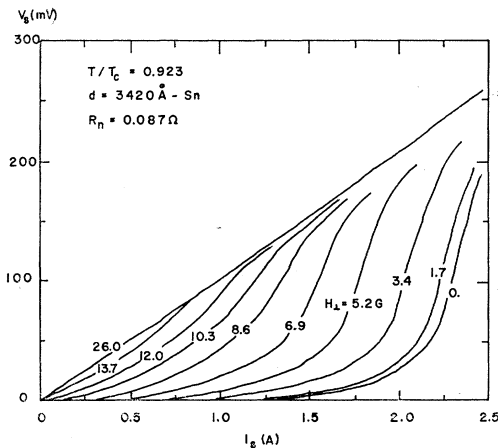


FIG. 11.  $V$ - $I$  characteristic as function of the magnetic field.

larger:

$$H_I^{\max} = \frac{0.2I}{w} \left( \ln \frac{w}{d} - 1 \right) = 0.869I \text{ G.} \quad (6)$$

For the thinner films this field component is proportionately smaller, since the current  $I$  used decreases linearly with film thickness  $d$ , while the factor increases only logarithmically with  $1/d$ .

It should be mentioned that the use of a current return other than the strip line configuration seems to result in more curvature of the  $V$ - $I$  curves than one would expect from the differences between Eq. (5) and Eq. (6).

For those films and temperatures where a linear region of the  $V$ - $I$  curves was found, the slope was used to define a flux-flow resistivity  $\rho_f$  by

$$\rho_f = dE/dJ = (wd/l)dV/dI, \quad (7)$$

where  $E$  is the electric field in the film and  $l$  the length of the film. The resulting values were normalized to the normal state resistivity  $\rho_n$ . Figure 12 shows that for  $T/T_c \geq 0.9$  and  $H_{\perp}/H_{c1}(T) \leq 0.45$  the normalized flow resistivity  $\rho_f/\rho_n$  varies with  $H_{\perp}/H_{c1}(T)$  as

$$\rho_f/\rho_n = 0.76 [H_{\perp}/H_{c1}(T)]^{3/2}. \quad (8)$$

Although this particular form of the equation has not been used, it is in good agreement with observations on bulk type-II samples<sup>3</sup> at about  $T/T_c = 0.9$  as shown in Fig. 13.

This apparent similarity of flux-flow behavior for both type-I films and bulk type-II superconductors should be contrasted by the order of magnitudes of some of the pertinent quantities in both cases.

Typical current densities reported<sup>5</sup> for bulk type-II samples are usually less than  $10^3$  A/cm<sup>2</sup>. In the present experiment flux flow has been observed up to about  $10^6$  A/cm<sup>2</sup>. Similarly, the linear portion of the  $V$ - $I$

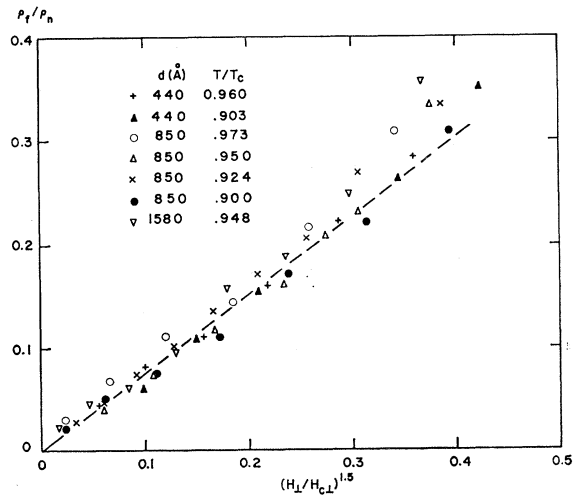


FIG. 12. Dependence of the reduced flow resistivity  $\rho_f/\rho_n$  on magnetic field.

curves in type-II materials is usually traceable up to a few mV, while in the pulsed-current experiments reported here, the linear portion has been traced up to 100 mV. The corresponding velocities of the flux tubes  $v_L$  are given by

$$v_L = cE/B, \tag{9}$$

where  $B$  is the magnetic induction.

At the large voltages and the low values of the perpendicular magnetic field used here, velocities up to  $10^5$  cm/sec are expected, while in typical bulk type-II superconductors values of the order of  $v_L \sim 10^2$  cm/sec are expected. Independent measurements<sup>26</sup> of the velocity of flux flow by a time-of-flight method has indeed confirmed velocities up to  $10^5$  cm/sec. The detailed dependence of  $v_L$  on  $H_L$  and  $J$ , however, was found to be different from that which would be expected from Eq. (9) and the present data, and shall be reported in a separate communication.<sup>27</sup>

### V. INSTABILITY CURRENT

All  $V-I$  curves in Figs. 6-11 show evidence of an increase in the slope  $dV/dI$  when the current is increased sufficiently. This increase was observed for all films tested. In general it is considerably sharper for low rather than high magnetic fields, regardless of film thickness or temperature. At the lowest temperatures this increase is extremely abrupt.

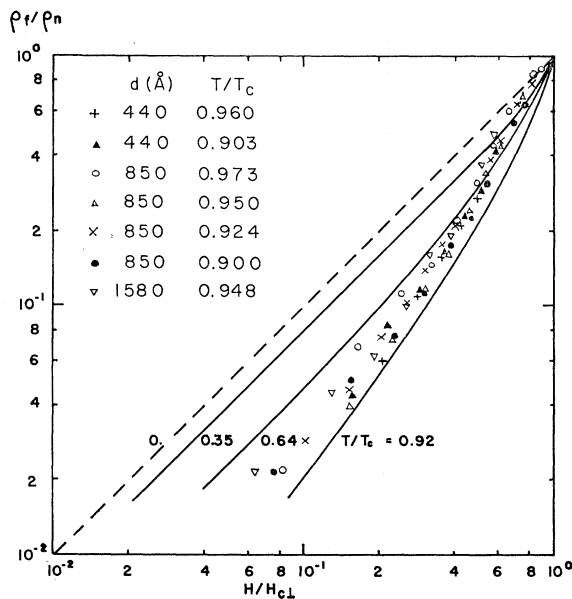


FIG. 13. Dependence of reduced flow resistivity  $\rho_f/\rho_n$  on magnetic field. Solid lines according to Ref. 3; data points, this experiment.

<sup>26</sup> Hans Meissner, in *Proceedings of the Eleventh International Conference on Low Temperature Physics*, edited by J. F. Allen *et al.* (University of St. Andrews Printing Department, St. Andrews, Scotland, 1969), Vol. II, p. 854.

<sup>27</sup> Hans Meissner, *J. Low Temp. Phys.* (to be published).

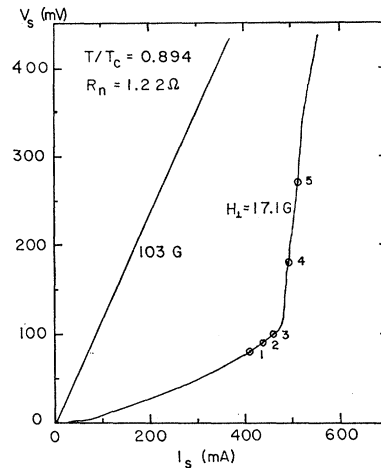


FIG. 14.  $V-I$  characteristic at  $t=70$  nsec. The numbered points refer to the numbered curves of Fig. 15. At  $H_L=103$  G the sample is fully normal conducting.

This sharp increase in sample resistance bears some resemblance to the thermally initiated instabilities which have been encountered in dc critical current experiments. As will be seen, however, this explanation can be ruled out for the present experiment.

Figures 14 and 15 show a comparison between a  $V-I$  curve and the corresponding  $V-t$  curves for five current pulse heights corresponding to the five numbered points along the  $V-I$  curve. The group of pulses has been chosen so as to straddle the onset of the instability. Points one, two, and three are in the linear flux-flow region, just below the onset of the instability.

The corresponding sample voltage pulses are flat. They rise with the current pulse, indicating that the flux flow starts promptly on a nanosecond time scale. Since the disturbing  $d\Phi/dt$  voltage can be found independently with a fully superconducting sample at  $H_L=0$ , it can be subtracted out and this result can be checked closely.

At point four, just beyond the sharp upward bend in the  $V-I$  curve, the sample voltage pulse is no longer flat but rises noticeably during the duration of the pulse. Another small increase in current (point five) brings a more rapid rise of the sample voltage. It is important,

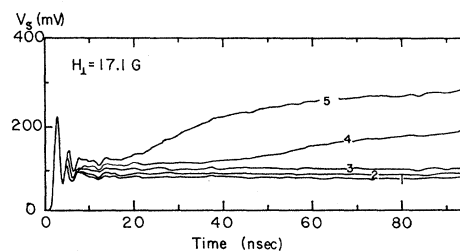


FIG. 15. Voltage-time characteristic for various current amplitudes. The numbered curves correspond to the numbered points of Fig. 14.

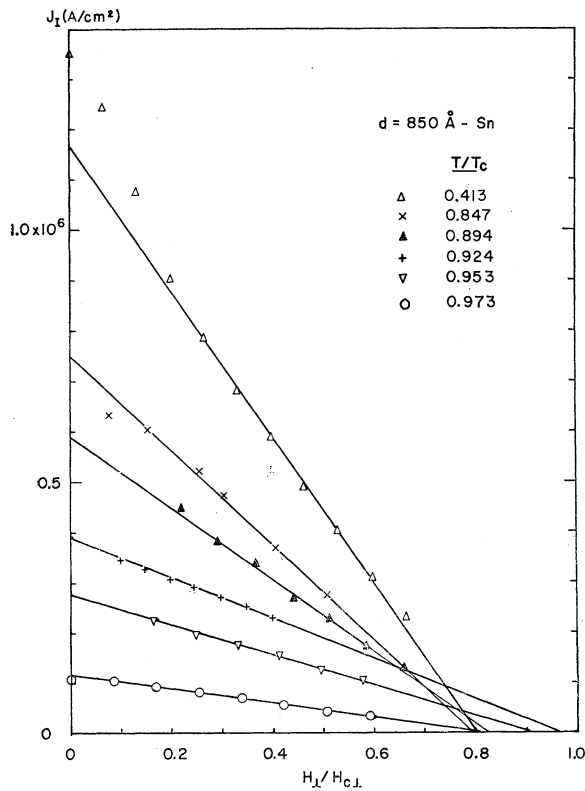


FIG. 16. Dependence of the instability current density  $J_I$  on magnetic field and temperature.

that the voltage then levels off at a value much smaller than  $IR_n$ .

This change in pulse shape provides a convenient criterion for the onset of the instability: The additional voltage  $\Delta V$  at  $t=80$  nsec is plotted as a function of  $I$ . The extrapolation to  $\Delta V=0$  defines the instability current  $I_I$  even for those cases where this point is not well marked on the  $V-I$  curves.

As shown in Fig. 16, the corresponding current density  $J_I$  has a simple dependence on the reduced magnetic field  $H_I/H_{c1}(T)$ :

$$J_I(H_I, T, d) = J_{I0}(T, d)[h_I - H_I/H_{c1}(T)], \quad (10)$$

where  $h_I$  varies between 0.8 and 0.96. The value of  $h_I$  depends on the definition of  $H_{c1}$ . As explained in Sec. III, lower values of  $H_{c1}$ , as might be found from the end of the magnetization curve rather than the onset of the resistance, would result in larger values of  $h_I$ . Thus, for theoretical considerations it seems justified to set  $h_I=1$ .

The dependence of  $J_{I0}$  on  $T/T_c$  and  $d$  is shown in Fig. 17 and Fig. 18. Near  $T_c$  the instability current  $J_{I0}$  is almost independent of thickness and is approximately given by

$$J_{I0} \approx 3 \times 10^6 [1 - (T/T_c)^2]. \quad (11)$$

## VI. DISCUSSION

The most important result of this investigation is the evidence that there are three current densities important for experiments with thin superconducting films,  $J_p$ ,  $J_I$ , and  $J_c$ . Since the true critical currents could not be observed in this investigation, only the first two will be discussed.

### A. Pinning Currents

The lowest of these three currents  $J_p$  is the current at which the flux tubes break free from pinning centers and at which the first voltage appears. (If there is some thermally activated flux creep, some small voltage may even appear at still lower currents.) In experiments with type-II superconductors this pinning current is usually denoted as the critical current.

It is tempting to construct a simple model for the understanding of  $J_p$ .  $J_p$  arises from the interplay between the Lorentz force on the flux tube  $J\phi_0/c$  and the pinning force. The latter can be estimated from the energetics of the magnetization curve. For thin type-I superconducting films in a perpendicular magnetic field, the magnetization near  $H_{c1}$  has been computed by

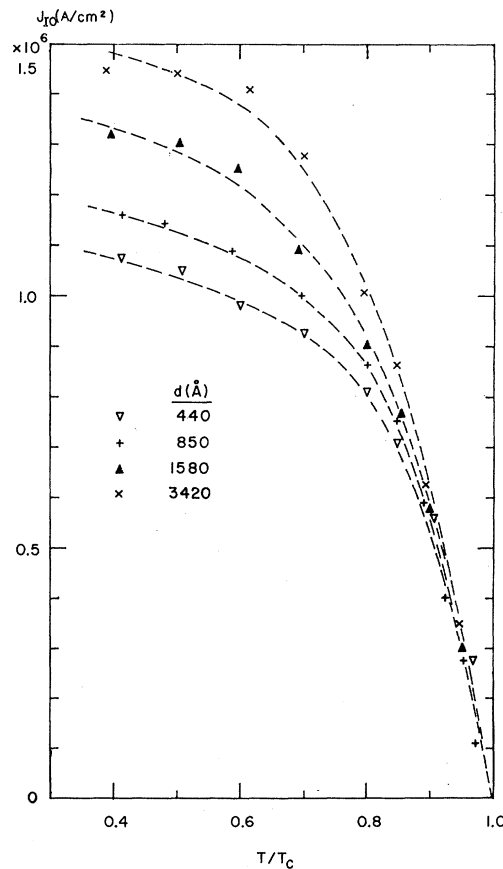


FIG. 17. Dependence of  $J_{I0}$  on temperature and film thickness.



Maki<sup>28</sup>:

$$-4\pi M = \frac{H_{c1} - H_1}{\beta[2\kappa^2 - f(\kappa d/\lambda)]}, \quad (12)$$

where  $\beta = \langle |\Psi|^4 \rangle_{av} / \langle |\Psi|^2 \rangle_{av}^2$  ( $= 1.159$  for a triangular flux tube lattice), and for  $\kappa d/\lambda \ll 1$

$$f(\kappa d/\lambda) = 0.7\kappa d/\lambda (2\pi)^{1/2}. \quad (13)$$

Here  $\kappa = \kappa(T)$  is the Ginzburg Landau constant and  $\lambda$  is the London penetration depth. Since  $\lambda$  depends on temperature as

$$\lambda = \lambda_0 [1 - (T/T_c)^4]^{-1/2}, \quad (14)$$

$f(\kappa d/\lambda) \rightarrow 0$  as  $T/T_c \rightarrow 1$ .

The difference of the Gibbs free energies of the film taken per unit volume is then given by

$$G_s - G_n = -\frac{H_c^2}{8\pi} + \frac{1}{4\pi} \int_0^{H_1} \frac{H_{c1} - H_1'}{\beta[2\kappa^2 - f(\kappa d/\lambda)]} dH_1', \quad (15)$$

where  $s$  is superconducting and  $n$  is normal.

Let us now calculate the energy difference  $\Delta G A d$  of a film of area  $A$  and thickness  $d$  when the field is decreased so that a single quantum of flux  $\varphi_0$  leaves the film. The necessary decrease in field  $\Delta H_1$  is given by

$$\Delta H_1 = -\varphi_0/A, \quad (16)$$

and the corresponding change in energy per unit length of flux line by

$$\epsilon = \Delta G A = -\frac{1}{4\pi} \frac{H_{c1} \varphi_0}{\beta[2\kappa^2 - f(\kappa d/\lambda)]} \left(1 - \frac{H_1}{H_{c1}}\right). \quad (17)$$

In the case above the flux line is expelled through a decrease of the field. Since forces between flux lines are mostly magnetic<sup>29</sup> they extend over a distance  $\lambda$  and the average force per unit length acting on the flux line is given by

$$\mathcal{F}_1 = \epsilon/\lambda. \quad (18)$$

Even assuming that the force acts over a distance  $\xi_{GL}$ , the Ginzburg-Landau coherence distance would not change the conclusions very much, since  $\xi_{GL}$  and  $\lambda$  have the same temperature dependence.

Instead of expelling the flux line by a decrease of field we will now consider expelling it by the Lorentz force acting on the pinned flux line:

$$\mathcal{F}_L = J_p \varphi_0 / c. \quad (19)$$

Equating the two forces gives

$$J_p = \frac{c}{4\pi \lambda \beta} \frac{H_{c1}}{[2\kappa^2 - f(\kappa d/\lambda)]} \left(1 - \frac{H_1}{H_{c1}}\right). \quad (20)$$

While the considerations above would be strictly valid only for a boundary against vacuum, it can be

<sup>28</sup> K. Maki, Ann. Phys. (N. Y.) **34**, 363 (1965).

<sup>29</sup> C. P. Bean and J. D. Livingston, Phys. Rev. Letters **12**, 14 (1964).

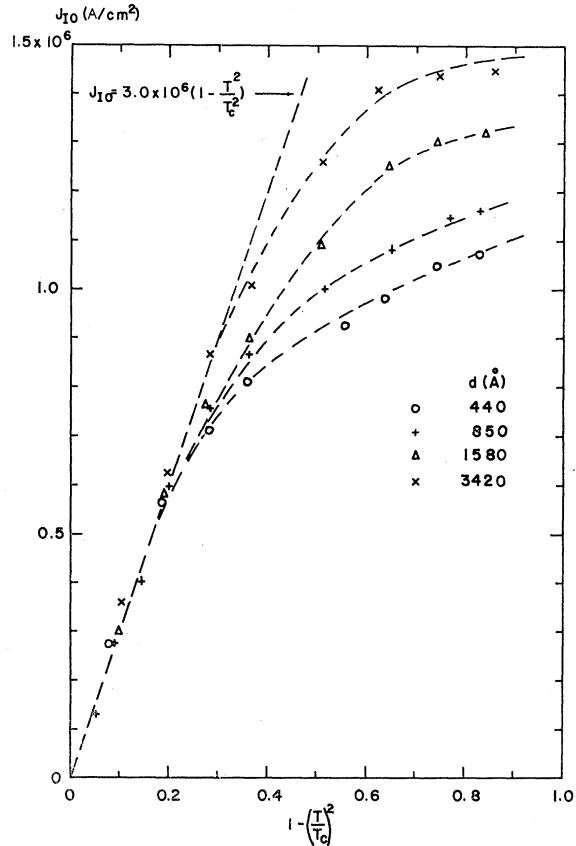


Fig. 18. Dependence of  $J_{10}$  on temperature and film thickness.

expected that, aside from a scaling factor, the same consideration applies also inside of the film.

In a thin film of  $d < \xi_{GL}$ , the flux cores have a diameter larger than the film thickness.<sup>30</sup> The crystal structure of the film shows grains with a size approximately equal to the film thickness. The grain boundaries thus go from one side of the film to the other and the crystal grains form boxes of about the right size for pinning a flux line.

Near  $H_{c1}$  Eq. (20) exhibits the experimentally observed field dependence. In general, one would expect that  $J_p$  would follow the magnetization curve, rising more sharply at low fields. This is indeed frequently the case. It is further corroborated by older data: Attempts at measuring the magnetization of thin films have very frequently resulted in magnetization curves which had the expected shapes, but which invariably gave magnetic moments much larger than those expected from theory. (See for instance Miller *et al.*<sup>31</sup> and Miller and Cody.<sup>17</sup>) In each case the magnetic moments were caused by pinned circulating currents and, in the terminology of this work, the measurement was equivalent to a determination of  $J_p$ . Cladis<sup>25</sup> also found similar

<sup>30</sup> P. Tholfsen and Hans Meissner, Phys. Rev. **169**, 413 (1968).

<sup>31</sup> P. B. Miller, B. W. Kington, and D. J. Quinn, Rev. Mod. Phys. **36**, 70 (1964).

results but used a somewhat different interpretation, originating with Deltour and Tinkham.<sup>32</sup>

The temperature dependence of  $J_p$  is more complex.  $H_{c1}$  is approximately given by

$$H_{c1} = \sqrt{2}\kappa(0)H_c(0)[1-t^2][1+t^2]^{-1}, \quad (21)$$

where  $t = T/T_c$ , while the temperature dependence of  $\kappa$  is approximately given by

$$\kappa = \kappa(0)/(1+t^2). \quad (22)$$

Together with the temperature dependence of  $\lambda$ , Eq. 14, we obtain

$$J_{p0} = \frac{c}{4\pi} \frac{H_c(0)}{\lambda(0)} \frac{(1-t^2)^{3/2}(1+t^2)^{3/2}}{1.159\sqrt{2}\kappa(0)[1-0.7d(1+t^2)^{3/2}(1-t^2)^{1/2}/2\kappa(0)\lambda(0)(2\pi)^{1/2}]}. \quad (23)$$

This temperature dependence agrees only very roughly with the experimental observations. Part of the lack of agreement may be caused by the approximation for  $f(\kappa d/\lambda)$  used in Eq. (13). This approximation is valid only for  $\kappa d/\lambda \ll 1$ . Since at the lower temperatures  $\kappa d/\lambda \approx 1$ , the use of this approximation becomes questionable.

With  $H_c(0) = 304.5 \text{ G} = 242.7 \text{ A/cm}$ ,  $\lambda(0) = 590 \text{ \AA}$  (for  $d = 440 \text{ \AA}$ ),  $\kappa(0) = 0.94$ , one finds from Eq. (23)  $J_{p0}^{\text{th}} = 2.67 \times 10^7 \text{ A/cm}^2$ , while experimentally one finds  $J_{p0}^{\text{exp}} \approx 1.2 \times 10^6 \text{ A/cm}^2$ . The reduction by about a factor of 20 is easily explained by the use of a boundary against vacuum in the model, while experimentally one has only grain boundaries for the pinning.

One observation, however, is explained by the model: The very weak thickness dependence of  $J_{p0}$ . In Eq. (23)  $J_{p0}$  depends on thickness mainly through  $\lambda$  and  $\kappa$ , both of which increase slowly with decreasing film thickness.<sup>17</sup>

The thicker films show quantitatively a different temperature dependence. From the work of Miller and Cody,<sup>16,17</sup> one expects that in a perpendicular field, the film has a domain structure rather than a fluxoid structure if the thickness is larger than about  $7\lambda$ . (The details of the structure are rather sensitive to the metallurgical state. For instance at low values of  $H_1$ , Träuble and Essmann<sup>33</sup> found for single crystal lead foils a fluxoid structure with 50 flux quanta per flux tube rather than a domain structure.)

The domain structure is given by Landau's models. For the thickest film used here,  $d = 3400 \text{ \AA}$ , we expect that the nonbranching model<sup>34</sup> applies, since the branching stops when the branches become thinner than  $\Delta$ , where  $\Delta$  is the surface energy parameter, defined by  $S = \Delta H_c^2/8\pi$ , and  $S$  is the surface energy between a normal and a superconducting domain. Numerically  $\Delta$  is about  $\Delta \approx \xi_{\text{GL}} - \lambda$ , where  $\xi_{\text{GL}}$  is the temperature dependent Ginzburg-Landau coherence distance.<sup>35</sup>

<sup>32</sup> R. Deltour and M. Tinkham, Phys. Rev. Letters **19**, 125 (1967).

<sup>33</sup> H. Träuble and U. Essmann, Phys. Status Solidi **25**, 395 (1968).

<sup>34</sup> L. Landau, Physik. Z. Sowjetunion, **11**, 129 (1937); see also L. D. Landau and E. M. Lifshitz, *Electrodynamics of Continuous Media* (Addison-Wesley Publishing Company, Inc., New York, 1960), p. 182 ff.

<sup>35</sup> V. L. Ginzburg and L. D. Landau, Zh. Eksperim. i Teor. Fiz. **20**, 1064 (1950) (untranslated).

In the nonbranching model the free energy per unit volume of a thin film of thickness  $d$  in a perpendicular field  $H_1$  is given by

$$F = \frac{H_c H_1}{4\pi} + \frac{H_c^2}{2\pi} \left[ \frac{\Delta}{d} \varphi(h) \right]^{1/2}, \quad (24)$$

where  $h = H_1/H_c$  and  $[\varphi(h)]^{1/2}$  has been calculated by Lifshitz and Sharvin.<sup>36</sup> Except for very small values of  $h$ ,  $[\varphi(h)]^{1/2}$  can be represented by

$$[\varphi(h)]^{1/2} = (1-h)h(0.7195 - 0.2498h) \\ = 0.7195h - 0.9693h^2 + 0.2498h^3, \quad h \geq 0.1 \quad (25)$$

while for  $h \leq 0.1$ ,

$$[\varphi(h)]^{1/2} = (h/\pi^{1/2})[\ln(0.56/h)]^{1/2}. \quad (26)$$

Let us see whether this model can be used to estimate the pinning currents for the thicker films. Let us assume that a film of thickness  $d$  with dimensions  $L_x$  and  $L_y$  is in the  $x$ - $y$  plane. Let us assume that the magnetic field points in the  $z$  direction and that the current flows in the  $y$  direction. Furthermore, let us assume that the domains are laminas, extending throughout the film in the  $y$  direction. The Landau model predicts that the sum of the width of the superconducting domains  $a_s$  plus the width of the normal domains  $a_n$  is given by

$$a_s + a_n/d = (\Delta/d)^{1/2} [\varphi(h)]^{-1/2}. \quad (27)$$

The total number of the domains in the film is then given by

$$N = L_x/(a_n + a_s) = (L_x/d)[d\varphi(h)/\Delta]^{1/2}. \quad (28)$$

$N$  has a broad maximum at about  $h = 0.4$  and goes to zero both for  $h = 1$  and  $h = 0$ . This means that over a fairly large part of the range of  $h$  the magnetization of the film is adjusted not by changing the number of domains, but by changing the relative sizes  $a_n/a_s$ .

As far as the flux flow and flux pinning is concerned, the appearance of the plate is the following: For  $h \lesssim 0.5$  there are normal domains in a superconducting matrix, while for  $h \gtrsim 0.5$  there are superconducting domains in a normal matrix. For small values of  $h$ , the motion of the

<sup>36</sup> E. M. Lifshitz and Yu. V. Sharvin, Dokl. Akad. Nauk SSSR **79**, 783 (1951) (untranslated).

normal domains is pinned, while for large values of  $h$  the superconducting domains are pinned.

The force on the sample as a whole is given by

$$\mathcal{F}_1 = (H_1 \bar{J}/c) L_x L_y d, \quad (29)$$

where

$$\bar{J} = I/L_x d \quad (30)$$

is the average current density. The force on each domain is then given by

$$\mathcal{F}_1/N = (H_1 \bar{J}/c) L_y d (\Delta d)^{1/2} [\varphi(h)]^{-1/2}. \quad (31)$$

This force becomes infinitely large for  $h=1$ , but not for  $h=0$ , since  $H_1 \rightarrow 0$  for  $h=H_1/H_c \rightarrow 0$ .

Since the magnetization adjusts the domains mainly by changing their relative sizes, we can expect that the force exerted by the current also first "squeezes the domains" to a minimum size. The energy, per domain, which corresponds to this minimum size is twice the surface energy:

$$\phi = (H_c^2/4\pi) \Delta L_y d. \quad (32)$$

Since the minimum distance is  $2\Delta$ , this energy must be expended over a distance of  $2\Delta$  and the corresponding force is

$$\mathcal{F}_2 = (H_c^2/8\pi) L_y d. \quad (33)$$

Equating the forces on the domains, Eq. (31) and Eq. (33) gives

$$\bar{J}_p = [cH_c/8\pi (\Delta d)^{1/2}] (H_c/H_1) [\varphi(h)]^{1/2} \quad (34)$$

or, with the use of Eq. (25),

$$\bar{J}_p = [cH_c/(\Delta d)^{1/2}] (1-h) (0.7195 - 0.2498h), \quad h \geq 0.1 \quad (35)$$

or, for the range of Eq. (26),

$$\bar{J}_p = [cH_c/(\Delta d)^{1/2}] \pi^{-1/2} [\ln(0.56/h)]^{1/2}, \quad h \leq 0.1. \quad (36)$$

The field dependence given by Eqs. (35) and (36) is rather similar to the field dependence for films with fluxoid structure and agrees roughly with experiment.

The temperature dependence is governed by

$$H_c/(\Delta d)^{1/2} = H_c(0) (1-t^2) (1-t^4)^{1/4} / [\Delta(0)d]^{1/2} \quad (37)$$

$$= H_c(0) (1-t^2)^{5/4} (1+t^2)^{1/4} / [\Delta(0)d]^{1/2}, \quad (38)$$

where it was assumed that  $\Delta$  has the temperature dependence of  $\lambda$ . The temperature dependence reproduces the general trend of the experiments reasonably well.

One may object that the model above is critically dependent on the assumption of laminae, extending the length of the sample in the direction of the current. Actually, closer inspection shows that this is not the case since the dimensions of the sample,  $L_x$  and  $L_y$ , disappear from the final expression.

Nevertheless both of the theoretical expressions, Eq. (20) and Eq. (34), are based on rather crude models, and while their general agreement with experiment is

gratifying, a close comparison does not seem to be worthwhile at this moment. In comparison with other experimental arrangements<sup>25</sup> one has to keep in mind that in the present model no account has been taken of the possibility that the lines of force may not be normal to the surface of the film, but may have a "kink" at the film, which would lead to additional force terms.

## B. Instability Currents

The second current of interest for thin films is the instability current  $J_I$ . At the present moment there is no theoretical basis for its discussion. An important result of this investigation is the evidence that the instability current involves a time-dependent process. There are many other studies, both static<sup>25</sup> as well as time-dependent<sup>27</sup> where this instability current has been observed without full realization of its nature. A complete account of the time dependence is in preparation elsewhere.<sup>38</sup> At this moment it shall only be mentioned that the experiments indicate that the voltage rise is associated with a time constant  $t'$  which near  $T_c$  is approximately given by

$$t' = t_0 \exp[-J/J_0 (1-T/T_c)^2 (1-H/H_c)], \quad (39)$$

where  $t_0$  and  $J_0$  are constants. The instability current  $J_I$  is then the current at which  $t'$  becomes shorter than the time of observation.

There are several reasons why simple heating can be ruled out as the reason for the instability. First of all, it is rather improbable that simple heating would result in a linear dependence on magnetic field. Secondly, the most abrupt instabilities, occurring at the lowest temperatures, take place at much smaller power levels than the corresponding instabilities at higher temperatures. Measurements of the flow velocity of the flux tubes<sup>27</sup> seem to indicate that close to the instability current, the flow velocity reaches the velocity of sound in the metal. If the instability current is exceeded, all flux motion stops. These conclusions are in agreement with conclusions drawn by Cladis,<sup>25</sup> who referred to the instability current as  $I_c$ .

## ACKNOWLEDGMENTS

This work was supported in part by the National Science Foundation, in part by the Stevens Cryogenics Center through a grant from the DOD Themis program. One of us (PT) held an NSF Traineeship. We also would like to thank Dr. Albert Schmid for illuminating discussions and Gunther Wirth for the operation of the helium liquefier.

We are grateful to the Office of Naval Research for the supply of helium gas.

<sup>27</sup> F. B. Hagedorn, Phys. Rev. Letters **12**, 322 (1964).

<sup>38</sup> Hans Meissner, J. Low Temp. Phys. (to be published).